

Simulation of current-induced microwave oscillation in geometrically confined domain wall.

Katsuyoshi Matsushita, Jun Sato, and Hiroshi Imamura

Nanotechnology Research Institute (NRI), Advanced Industrial Science and Technology (AIST), AIST Tsukuba Central 2, Tsukuba, Ibaraki 305-8568, Japan.

We studied magnetization dynamics of a geometrically confined domain wall under dc current by solving simultaneously the Landau-Lifshitz-Gilbert equation and diffusion equation for spin accumulation. We showed that the oscillation motion of the domain wall is driven by the spin-transfer torque and the dc current is converted to the ac voltage signal. The results means that the geometrically confined domain wall is applicable as a source of microwave oscillator.

Achievement of a nano spin-transfer oscillator is one of important issues in microwave technology. Many studies have succeeded in development of microwave oscillation in nanopillars and point contacts[1, 2, 3, 4, 5, 6, 7, 8]. Recently possibilities of another kind of nano spin-transfer oscillators using a domain wall were proposed[9, 10]. In those works, the oscillation generating microwave in GMR or TMR devices is not an uniform oscillation of the free layer magnetization but an oscillation[9] or magnetization rotational motion[10] of the domain wall.

On the other hand, it is known that the resistance due to the domain wall depends on its magnetic structure[11, 12, 13]. If the oscillation motion of the magnetic structure of the domain wall is induced by spin transfer torque under dc current, we can obtain the ac voltage signal and can use the domain wall as a microwave source.

In this paper, we numerically calculate the dynamics of the geometrically confined domain wall [14] under the dc current by solving simultaneously the Landau-Lifshitz-Gilbert equation and diffusion equation for spin accumulation. We show that the oscillation of the magnetization vector of the domain wall is induced by the spin-transfer torque and we can obtain the ac voltage signal due to the domain wall oscillation. We also show that the power spectrum of the MR ratio has a sharp peak corresponding to the oscillation of the domain wall. The frequency of the peak is about 1 hundred GHz for the current density of about 0.01 mA/nm² which is reachable value in experiments with avoiding breakdown by Joule heating.

The system, we consider, is shown in Fig. 1. The system consists of two magnetic electrode layers and a non-magnetic insulator layer sandwiched by the electrodes. The insulator layer contains magnetic bridge which geometrically confines a domain wall. The system is divided into about 1500 hexahedral finite elements, where spin accumulation and demagnetization field are evaluated. The size of magnetic metal electrode at the bottom and top layers is 8 × 8 × 4 nm. The shape of the bridge between two electrodes is a rotated elliptic arch around the center axis perpendicular to the layers, the diameters of the bottom and center layers of which are set at 6 and 4 nm, respectively. The size of the system is larger than the diffusion length of 2nm of CoFe[15] at room temperatures. Thus we can deal with the electron system in diffusive limit, unlike a previous ballistic treatment[16].

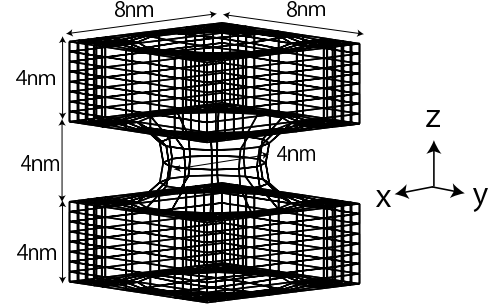


FIG. 1: The model of a geometrically confined domain wall for a finite element method.

Then as previously predicted by Šimánek[13], the spin accumulation mainly induces domain wall resistance.

The magnetization vectors are expressed by the classical spins on the simple cubic lattice with the lattice constant of $a = 0.4\text{nm}$. The Hamiltonian \mathcal{H} is given by

$$\mathcal{H} = -J_{\text{dd}} \sum_{\langle i,j \rangle} \vec{S}_i \cdot \vec{S}_j + J_{\text{sd}} \sum_i \vec{S}_i \cdot \delta \vec{m}_i + \frac{K_d}{4\pi} \sum_i \vec{S}_i \cdot \int d\vec{r} \left\{ \frac{\hat{1}}{|\vec{r}_i|^3} - 3 \frac{\vec{r}_i \otimes \vec{r}_i}{|\vec{r}_i|^5} \right\} \cdot \vec{S}(\vec{r}), \quad (1)$$

where \vec{r}_i represents the relative coordinate of the i -th site from the position \vec{r} , \vec{S}_i , the classical Heisenberg spin with absolute value of unity and, $\delta \vec{m}_i$, local spin accumulation density at the i -th site. Such the semi-classical treatment is justified for the system with ferromagnetic order because the magnetization is larger than its quantum fluctuation. The first and second terms in the right hand side of Eq. (1) express the exchange interactions between local magnetizations at nearest neighbor sites, and between local magnetization and spin accumulation at each site, respectively. The exchange coupling constant between nearest local magnetization denoted by J_{dd} is related to the exchange stiffness constant in continuous limit, A , and a lattice constant, a , with $J_{\text{dd}} = 2aA$. We set J_{dd} at 0.04 eV which is on the order of the transition temperature of CoFe, $T_c \sim 1.2 \times 10^3 K$. The exchange coupling constant J_{sd} is set at 0.1 eV in accordance with Ref.[17]. The third term denotes the dipole-dipole in-

interaction energy. In order to deal with the dipole-dipole interaction in a complex system shape, we adopt a finite element - boundary element (FEM-BEM) hybrid method [18] on the spin field on the continuum space, $\vec{S}(\vec{r})$, which is defined for each position, \vec{r} , by the spin field extrapolated from the lattice sites to the position. The exchange length for the dipole-dipole interaction is $l_{\text{ex}} = \sqrt{J_{\text{dd}}/2K_d} \sim 3$ nm, which is comparable to the length of the considered confining region of 4nm. Thus the thickness of the domain wall depends on both the size of the confining region and the exchange length.

In the adiabatic approximation, the local spin accumulation density, $\delta\vec{m}_i$, is determined by solving the following differential equations[17],

$$\frac{\partial}{\partial t} \delta\vec{m}(\vec{r}) = \nabla \left\{ \beta \vec{S}(\vec{r}) \vec{j}_e(\vec{r}) + \hat{A}(\vec{S}(\vec{r})) \delta\vec{m}(\vec{r}) \right\} + \frac{J_{\text{sd}}}{\hbar} \delta\vec{m}(\vec{r}) \times \vec{S}(\vec{r}) + \frac{\delta\vec{m}(\vec{r})}{\tau}, \quad (2)$$

$$\hat{A}(\vec{S}(\vec{r})) = 2D_0 \left[\hat{1} - \beta^2 \vec{S}(\vec{r}) \otimes \vec{S}(\vec{r}) \nabla \right], \quad (3)$$

where \vec{j}_e , C_0 , D_0 , β and τ denote electronic current, conductivity, diffusion constant, polarization of resistivity and relaxation time due to a spin-orbit interaction respectively. Equations (2)-(3) are solved numerically with combining continuous equation for electronic current, $\nabla \vec{j}_e = 0$. C_0 and β are taken to be those for conventional ferromagnets as $C_0 = 70\Omega\text{nm}$ and $\beta = 0.65$, respectively. D_0 and τ are obtained, respectively, by the Einstein relation, $C_0 = 2e^2 N_{\text{F}} D_0$ and $\lambda = \sqrt{2\tau D_0 (1 - \beta^2)}$ for given diffusion length λ , density of states at the Fermi level, N_{F} and electron charge e . Here we employ $\lambda = 12\text{nm}$ and $N_{\text{F}} = 7.5\text{nm}^{-3} \text{eV}^{-1}$. For the boundary condition of the spin accumulation, we artificially adopt $\delta\vec{m} = \vec{0}$ at the top and bottom layers, ignoring any parasitic resistance. On the other boundaries, the natural boundary condition is employed. In the case, the simulated spin accumulation distribution is nonuniform and concentrate on the contact region.

Substituting the solution of Eqs. (2) and (3) into Eq. (1), we evaluate the Hamiltonian of Eq. (1). The effective magnetic field for \vec{S}_i is given by $\partial\mathcal{H}/\partial\vec{S}_i$ and the dynamics of \vec{S}_i is determined by the following Landau-Lifshitz-Gilbert equation,

$$\frac{d}{dt} \vec{S}_i = \frac{\gamma}{1 + \alpha^2} \vec{S}_i \times \left(\frac{\partial\mathcal{H}}{\partial\vec{S}_i} + \alpha \vec{S}_i \times \frac{\partial\mathcal{H}}{\partial\vec{S}_i} \right), \quad (4)$$

where γ and α denote the gyromagnetic ratio and the Gilbert damping constant. The equation is numerically solved by a quaternion method[19]. The time step Δt and α are set at 3.4×10^{-2} fs and 0.02, respectively. The number of sites, N_s is about 10^4 . For simplicity, we use antiparallel boundary condition of the spins in order to simulate the experimental situation with a 180° domain wall. On the boundary, \vec{S}_i 's are fixed at $(-1,0,0)$ on the top electrode and $(+1,0,0)$ on the bottom electrode except for the boundary surface between the magnetic

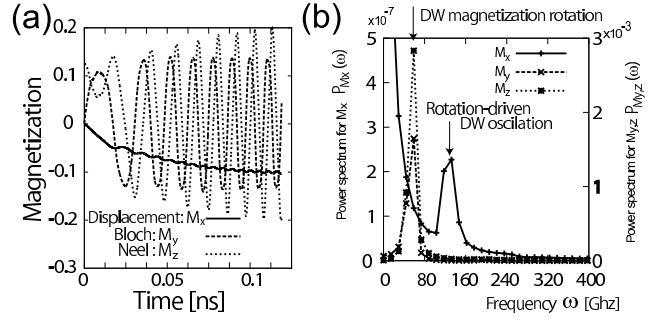


FIG. 2: (a) The x , y , and z -components of the mean magnetization vector, \vec{M} , is plotted as a function of time t for $j = 0.012\text{mA}/\text{nm}^2$ (b) The power spectra of the magnetization, $P_{x,y,z}$, are plotted as a function of frequency ω .

and insulator layers. The directions of spins, x , y and z are defined as shown in Fig. 1.

In the present work, we employ current of $0.012\text{mA}/\text{nm}^2$. The current is applied in the perpendicular direction to the layers. The simulation starts from stable Néel wall state obtained by a simulation without dc current density.

In order to understand dynamics of the local magnetization distribution of the domain wall, we calculate the magnetization $\vec{M} = (\sum_i \vec{S}_i) / N_s$ for the whole of the system. The typical result in time dependence of the magnetization is shown in Fig. 2(a). We observe steady regular rotation around the x -axis. Such rotation is known for the moving domain wall in wire systems above Walker's threshold current[20]. The magnetic structures with $M_y = 0$ and $M_z = 0$ correspond to the Néel wall and the Bloch wall, respectively. Thus the rotation corresponds to an oscillation between the Néel and Bloch walls. On the other hand, the displacement of the domain wall center is characterized by the value of M_x because the magnetization vectors at the boundary surface are aligned to be parallel to the x -axis. As shown in Fig.2(a) that the domain wall displacement oscillates as a function of time.

Figure 2(b) shows the power spectra of the magnetization motions, which are defined by

$$P_{x,y,z}(\omega) = \frac{1}{T} \iint_{T_0}^{T_0+T} e^{-i\omega t} M_{x,y,z}(\tau) M_{x,y,z}(t - \tau) d\tau dt, \quad (5)$$

where T_0 and T are much longer than the periods of the oscillations. Each spectrum has a single characteristic frequency. The frequency of the displacement oscillation is twice of that of the rotational motion. This is because the displacement oscillation originates from coupling with the rotational motion driven by the spin transfer torque. For the Néel and Bloch walls, respectively, the displacement takes minimum and maximum.

The oscillation of the magnetization vectors induces the oscillation of the spin accumulation through Eq. (2).

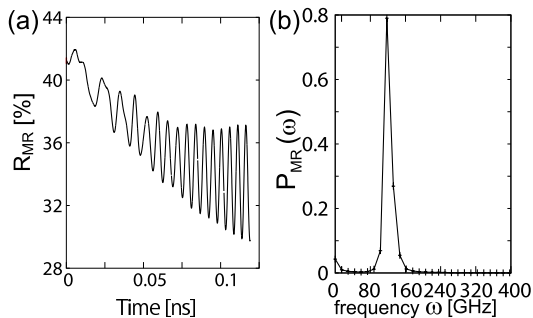


FIG. 3: (a) The magnetoresistance ratio R_{MR} is plotted as a function of time t for $0.01\text{mA}/\text{nm}^2$. (b) The power spectrum of the magnetoresistance ratio P_{MR} is plotted as a function of frequency ω .

The electric field at position \vec{r} is given by

$$\vec{E}(\vec{r}) = \frac{1}{2C_0} \left(\vec{j}_e(\vec{r}) + 2D_0 \left[\hat{1} + \beta\vec{\sigma} \cdot \vec{S}(\vec{r}) \right] \delta\vec{m}(\vec{r}) \right). \quad (6)$$

The voltage drop of the system is obtained by integrating the electric field $\vec{E}(\vec{r})$ along z -axis. From Eq. (6), the oscillation in the spin accumulation then yields the oscillation in magnetoresistance ratio, $R_{MR}(t) = R(t)/R_0 - 1$, where R_0 and $R(t)$ denote resistance with and without a domain wall, respectively. R_{MR} oscillates as a function of time t as shown in Fig. 3(a). The power spectrum of R_{MR} defined by

$$P_{MR}(\omega) = \frac{1}{T} \iint_{T_0}^{T_0+T} e^{-i\omega t} R_{MR}(\tau) R_{MR}(t - \tau) d\tau dt \quad (7)$$

is shown in Fig. 3(b). In the accuracy of our calculation,

P_{MR} has a characteristic isolated peak. Thus the dc current is converted to the ac voltage signal with a characteristic frequency. The frequency of the peak agrees with that of the P_x denoted by the arrow in Fig 2(b). Thus the MR oscillation is due to periodically change of the spin accumulation induced by the displacement oscillation.

We note that only the resistance due to the spin accumulation is considered. However in the real system the resistance originates from not only the spin accumulation but also scattering of electrons due to the domain wall[11, 12]. The correction will enhance the magnetoresistance ratio and therefore the power of the microwave oscillation as compared with the results of our simulation.

In conclusion, we studied the magnetization dynamics of the geometrically confined domain wall under dc current by solving the Landau-Lifshitz-Gilbert equation and diffusion equation for the spin accumulation. From calculation result, we propose a scenario of the microwave generation as follows: current induced spin-transfer torque drives magnetization rotation in the domain wall. Then the displacement oscillation of domain wall is induced by the coupling with the rotation and drives spin accumulation oscillation. As a result the microwave oscillation in voltage signal appears. We conclude that the geometrically confined domain wall is applicable as a source of microwave generator.

The authors would like to thank M. Doi, H. Iwasaki, M. Ichimura, M. Takagishi, M. Sahashi, M. Sasaki, T. Taniguchi, N. Yokoshi and K. Seki for useful discussions. The work was supported by The New Energy and Industrial Technology Development Organization (NEDO). K. M. was supported by a Grant-in-Aid for Young Scientists from the Ministry of Education, Science, Sports and Culture of Japan.

-
- [1] J. A. Katine, F. J. Albert, R. A. Buhrman, E. B. Myers, and D. C. Ralph, *Nature* **84**, 4212 (2000).
 - [2] M. Tsoi, A. G. M. Jansen, J. Bass, W.-C. Chiang, V. Tsoi, and P. Wyder, *Nature* **406**, 46 (2000).
 - [3] S. I. Kiselev, J. C. Sankey, I. N. Krivorotov, N. C. Emley, R. J. Schoelkopf, R. A. Buhrman, and D. C. Ralph, *Nature* **425**, 380 (2003).
 - [4] W. H. Rippard, M. R. Pufall, S. Kaka, S. E. Russek, and T. J. Silva, *Phys. Rev. Lett.* **92**, 027201 (2004).
 - [5] M. Covington, M. A. H. Darwish, Y. Ding, N. J. Gokemejier, and M. Seigler, *Phys. Rev. B* **69**, 184406 (2004).
 - [6] I. N. Krivorotov, N. C. Emley, J. C. Sankey, S. I. Kiselev, D. C. Raph, and R. A. Buhrman, *Science* **307**, 228 (2005).
 - [7] S. Kaka, M. R. Pufall, W. H. Rippard, T. J. Silva, S. E. Russek, and J. A. Katine, *Nature* **437**, 389 (2005).
 - [8] F. B. Mancoff, N. D. Rizzo, B. N. Engel, and S. Tehrani, *Nature* **437**, 393 (2005).
 - [9] J. He and S. Zhang, *Appl. Phys. Lett.* **90**, 142508 (2007).
 - [10] T. Ono and Y. Nakatani, *Appl. Phys. Exp.* **1**, 061301 (2008).
 - [11] P. M. Levy and S. Zhang, *Phys. Rev. Lett.* **79**, 5110 (1997).
 - [12] A. Brataas, G. Tatara, and G. E. W. Bauer, **60**, 3406 (1999).
 - [13] E. Šimánek, **63**, 224412 (2001).
 - [14] P. Bruno, *Phys. Rev. Lett.* **83**, 2425 (1999).
 - [15] S. M. Moyerman, J. G. Checkelsky, S. S. Harberger, A. C. Tamboli, M. J. Carey, P. D. Sparks, and J. C. Eckert, **97**, 10C513 (2005).
 - [16] J. i. Ohe and B. Kramer, **96**, 027204 (2006).
 - [17] S. Zhang, P. M. Levy, and A. Fert, *Phys. Rev. Lett.* **88**, 236601 (2002).
 - [18] D. R. Fredkin and T. R. Koehler, **26**, 415 (1990).
 - [19] B. Visscher and X. Feng, **65**, 104412 (2002).
 - [20] G. Tatara and H. Kohno, *Phys. Rev. Lett.* **67**, 113316 (2004).